AD NUMBER

AD810470

NEW LIMITATION CHANGE

TO

Approved for public release, distribution unlimited

FROM

Distribution authorized to U.S. Gov't. agencies and their contractors; Critical Technology; 13 JAN 1967. Other requests shall be referred to Naval Ordnance Labatory, White Oak, Silver Spring, MD.

AUTHORITY

NOL ltr, 15 Nov 1971

NOLTR 66-150

NUMERICAL HYDRODYNAMIC CALCULATIONS OF THE FLOW OF THE DETONATION PRODUCTS FROM A POINT-INITIATED EXPLOSIVE CYLINDER

13 JANUARY 1967

NOL

UNITED STATES NAVAL ORDNANCE LABORATORY, WHITE OAK, MARYLAND

NOLTR 66-150

NUMERICAL HYDRODYNAMIC CALCULATIONS OF THE FLOW OF THE DETONATION PRODUCTS FROM A POINT-INITIATED EXPLOSIVE CYLINDER

By

D. Piacesi, Jr.

ABSTRACT: With the use of the NOL two-dimensional hydrodynamics computer program (CYCLONE), a detailed numerical analysis is made of the flow in the product-gas of a detonating cylinder of pentolite (50/50 PETN/TNT) explosive. The explosive cylinder is initiated at a point on the central charge axis at one end-face. The detonation front is assumed to be spherical. This is consistent with experimentally determined wave shapes. The calculations are carried out to the point where the detonation front is at 1.71-charge-diameters from the point of initiation. The results of the calculations show that the flow in the "detonation head" (region bounded by the detonation front, and the lateral and rear rarefaction waves) is entirely spherical. Moreover, this spherical flow is exactly that which is described by the similarity solution of G. I. Taylor for a spherical detonation wave.

EXPLOSION DYNAMICS DIVISION
EXPLOSIONS RESEARCH DEPARTMENT
U. S. NAVAL ORDNANCE LABORATORY
WHITE OAK, MARYLAND

NOLTR 66-150 13 January 1967

NUMERICAL HYDRODYNAMIC CALCULATIONS OF THE FLOW OF THE DETONATION PRODUCTS FROM A POINT-INITIATED EXPLOSIVE CYLINDER

This report discusses the results of numerical hydrodynamic calculations on the flow in the product-gas resulting from the detonation of a cylinder of explosive. This report will be of interest to scientists who are dealing with experiments involving point-initiated explosive cylinders, and to engineers concerned with conventional explosive weapons design. This work was carried out under NAVORD Task ORD-033-221/092-1/F008-08-11 Problem 004 - Explosion Hydrodynamic Calculations.

E. F. SCHREITER
Captain, USN
Commander

C. J. Aronson

C. J. ARONSON
By direction

CONTENTS

ILLUSTRATIONS

I. INTRODUCTION

Let us examine the flow produced by the detonation of an unconfined right circular cylinder of high explosive, where the initiation is at a point on the central axis at one end-face (refer to Fig. 1). As the detonation progresses from the point of initiation, the gaseous explosion products expand out through the end-face. Consequently, a rarefaction wave travels into the gas behind the detonation front. When the detonation reaches the side of the cylinder, a shock is transmitted into the surrounding medium and a lateral rarefaction wave is reflected into the explosion products. Subsequently, the head of the lateral rarefaction wave impinges on the central charge axis and annihilates the rear rarefaction wave. The region bounded by the head of the lateral rarefaction and the detonation front is sometimes referred to as the "detonation head".[1]*

While considerable attention has been given to the detonation head, there does not appear to be in the literature any attempt to calculate the actual flow in the detonation head region. With the use of the Naval Ordnance Laboratory's two-dimensional hydrodynamics computer program, CYCLONE[2], a detailed numerical analysis of this transient compressible flow problem can be carried out. The results of calculations for a two-inch diameter cylinder of pentolite (50/50 PETN/TNT) explosive are presented in Sec. V of this report. The calculations were performed on an IBM-7090 computer.

* References are on Page 15.

II. THE PHYSICAL MODEL

We make the physical assumptions about the detonation that (1) the chemical reaction zone is infinitely thin (i. e., the solid explosive is instantaneously converted to gaseous products as the shock-detonation front passes over it), (2) the Chapman-Jouguet (CJ) conditions[3] hold at the detonation front, (3) the detonation propagates in all directions from the point of initiation with the CJ detonation velocity,* (4) the explosive is surrounded by a vacuum, and (5) "edge" effects are negligible. Here, the term "edge"effects refers to the radical change in the curvature of the detonation front near the cylindrical surface of the charge. This effect is produced by the influence of the lateral rarefaction wave on the chemical reaction zone.

In solid high explosives, the width of the chemical reaction zone is of the order of several millimeters and therefore assumption (1) does not impose a too unreal restriction on the physical model. Assumption (1) does, however, eliminate any effect of the lateral rarefaction wave on the chemical reaction zone at the sides of the cylinder. Hence, assumption (5) results as a natural consequence of (1). In the experiments by Cook, et al.[1], the edge effect did not exceed 2 mm in any case. Assumption (2) is introduced into the calculations via the equation of state of the detonation-product gas (see Sec. IV).

* The CJ detonation velocity is defined as $D = V_1 [(p_2 - p_1)/(V_1 - V_2)]^{\frac{1}{2}}$, where p_1, V_1 (p = pressure, V = specific volume) is the initial state of the solid unreacted explosive and p_2, V_2 is the point of tangency of the Rayleigh line from P_1, V_1 to the reactive Hugoniot of the product gas. This is the theoretical maximum steady-state velocity which the detonation can achieve. See Ref. (3).

The shape of the detonation front directly affects the flow in the region behind the wave front. Assumption (3) imposes the requirement that the wave front coincide with the surface of an expanding sphere, whose radius of curvature is equal to the product of the CJ detonation velocity (D_{CJ}) and the time (t) elapsed after initiation. Cook, et al.,[1] and Jaffe and Clairmont[4], show experimentally that in point-initiated cylinders of "ideal" explosives* the detonation front is indeed initially spherical, and that the radius of curvature of the front is $D_{CJ}t$. However, there is a fundamental difference between the two sets of data. In the work by Cook et al., the radius of curvature of the detonation front approaches a constant value by the time the wave has propagated a distance of less than four charge diameters from the point of initiation. From this point on, the detonation front propagates in a "steady state" condition. In the experimental work by Jaffe and Clairmont with two-inch diameter tetryl cylinders, the radius of curvature of the detonation front increases geometrically (radius = $D_{CJ}t$) at a distance of four charge diameters from the point of initiation with no indication of reaching a steady state. In the computer calculations which are described in this report, the mathematical model of the detonation is consistent with both sets of data, since the calculations were only carried out until the detonation front is at 1.71 charge diameters from the point of initiation. There is, however, an obvious extrapolation of the calculations which can be made in the light of the Jaffe-Clairmont experimental results. This is done in Sec. VI.

* We define an "ideal" explosive as one in which the detonation propagates at the theoretical maximum steady-state velocity (i.e., the CJ detonation velocity).

III. THE HYDRODYNAMIC EQUATIONS AND THE MATHEMATICAL MODEL

We can write the hydrodynamic equations for transient, isentropic, axially symmetric flow in Lagrangian form as follows: Denote the Lagrangian coordinates by k, l, the Eulerian coordinates by R,Z, the velocity components by u, v, the density by ρ, the specific volume by $V = (1/\rho)$, the internal energy by E, the pressure by p, and the time by t. Then the equations are

(continuity)
$$\frac{\rho_0}{\rho} = \frac{RA}{R_0 A_0}, \tag{1}$$

where
$$A = \frac{\partial(R,Z)}{\partial(k,l)}, \tag{2}$$

(momentum)
$$\frac{d^2R}{dt^2} = \frac{-R}{\rho_0 R_0 A_0}\left[\frac{\partial p}{\partial k}\frac{\partial Z}{\partial l} - \frac{\partial p}{\partial l}\frac{\partial Z}{\partial k}\right], \tag{3}$$

$$\frac{d^2Z}{dt^2} = \frac{-R}{\rho_0 R_0 A_0}\left[\frac{\partial p}{\partial l}\frac{\partial R}{\partial k} - \frac{\partial p}{\partial k}\frac{\partial R}{\partial l}\right], \tag{4}$$

$$u = \frac{dR}{dt} = \int \frac{d^2R}{dt^2}\,dt, \quad v = \frac{dZ}{dt} = \int \frac{d^2Z}{dt^2}\,dt,$$

$$R = \int \frac{dR}{dt}\,dt, \quad Z = \int \frac{dZ}{dt}\,dt,$$

(energy)
$$\frac{\partial E}{\partial t} = -p\frac{\partial V}{\partial t} \tag{5}$$

where the subscript zero refers to the initial state of the material. The equation of state for each material is assumed given in the form $p = p(E,V)$.

The von Neumann-Richtmyer finite difference method,[4] which handles shocks automatically, is used for the numerical integration of the hydrodynamic equations. In this scheme, an artificial

dissipative term is introduced into the conservation of energy and momentum equations. This term causes shocks to have a finite thickness and makes the flow variables change abruptly but continuously through the region of the shock. In addition, the correct entropy change is effected across the shock. In CYCLONE, the artificial dissipative term is defined as

$$q = \frac{b A}{V V_0^2}\left(\frac{\partial V}{\partial t}\right)^2 \qquad (6)$$

where the variables A, V, and t are defined above and b is the shock-width constant, which can be adjusted to give the desired sharpness to the shock. The pressure, p, in equations (3), (4), and (5) is then replaced by $P = (p+q)$. The finite difference analogues of the hydrodynamic equations which are actually used in the numerical integration, can be found in Ref. 2.

Let us now briefly examine the mathematical model that is used in the finite difference method. As a result of the cylindrical symmetry, the three-dimensional flow can be represented by the flow in any R, Z ($R \geq 0$, θ = const) half plane (Fig. 2). Lagrangian coordinate (k,l) lines, imbedded in the material, divide the material into zones. Initially, the mass of each zone is calculated. This mass remains constant throughout the computations, thus assuring conservation of mass. There is then assigned to each mesh point (intersection of a k and an l line) a mass equal to one-fourth of the mass in the four surrounding zones. The velocity components of each

mass point and the pressure, internal energy, and density of each zone are given as initial conditions.

At each computation cycle, the program calculates consecutively for each zone ρ from the continuity equation, E and p from the simultaneous solution of the energy equation and the equation of state, and q from the formula given in eq. (6). At this point, a time step for the integration is determined from stability conditions.[6] The accelerations of each of the mass points are next determined by the momentum equations. From the accelerations and the time step, the new velocity components and positions of the mass points are then obtained. The calculations are advanced in finite increments of time by repeating the above steps at every integration cycle. The material flow is thus determined by the motion of the mass points.

A programmed detonation scheme is used to instantaneously convert the solid high explosive to gaseous explosion products. Since we assume the detonation propagates with the constant CJ velocity from the point of initiation, we therefore can calculate the position of the detonation surface at each computation cycle. For each zone containing solid explosive, a test is made to see if the detonation front has arrived at the zone (corner nearest the point of initiation). If it has arrived, the chemical energy of the solid explosive which is contained in the zone is added to the internal energy of that zone*. For this and subsequent time cycles, this zone uses the equation of state for the gaseous explosion products. If the detonation has not

* In the reported calculations (Sec. V), the chemical energy was actually added in discrete amounts of 1/3 the total chemical energy in the zone as the detonation front passed over each 1/3 section of the diagonal of the zone. By allowing the energy adjustment to take place over several computation cycles, the typical oscillations found in numerical calculations of this type were greatly reduced.

yet arrived, the equation of state of the solid unreacted explosive is used.

IV. EQUATIONS OF STATE

In compressible fluid flow calculations, it is necessary to have an equation of state for each material. The equations of state which are used for the solid unreacted explosive and the detonation product gases are discussed in this section.

When making numerical hydrodynamic calculations, it is often a satisfactory approximation, at least for solids, to use the shock Hugoniot (the locus of possible states which are attainable from some initial state by a single shock transition) as an equation of state. The equation of state for the solid unreacted Pentolite explosive is taken as

$$p = 0.1282\ \mu + 1.193\ \mu^3, \qquad (7)$$

where p is the pressure (megabars), $\mu = \rho/\rho_o - 1$, and ρ is the density (g/cm^3). The subscript zero refers to the initial state. Equation (7) may not closely represent the shock Hugoniot for unreacted pentolite. It is probably more representative of the shock Hugoniot for unreacted Composition B explosive (see, for example, Ref. (7)). However, almost any reasonable form for the equation of state is adequate for our calculations since the detonation is programmed as a function of time and does not depend on the state of the solid explosive. The form of the equation of state for the solid explosive has essentially no effect on the flow in the detonation-product gases.

The equation of state of the pentolite detonation-product gas is assumed to be given in the form[8]

$$p = (A\rho + B\rho^2)\ E + C\rho^3 \qquad (8)$$

where A, B, and C are constants and p, E, and ρ are the thermodynamic variables described above. The value A = 0.35 is obtained by defining $A = (\gamma - 1)$, where γ is the average ideal gas specific heat ratios (c_p/c_v) of the detonation products. Equation (8) thus approaches the polytropic gas equation for small ρ. The constants B = 0.1243 and C = 0.01279 were chosen so that eq. (8) would reproduce the particular CJ detonation conditions and the CJ isentrope obtained by thermochemical calculations.*

The CJ detonation conditions for pentolite (ρ_o = 1.65) gotten with the thermochemical calculations are pressure p_{CJ} = 0.2452 megabars, density ρ_{CJ} = 2.210 g/cm^3, sound speed c_{CJ} = 0.5714 cm/μsec, and detonation velocity D = 0.7655 cm/μsec. The value of the CJ specific internal energy E_{CJ} = 0.0775 megabar-cm^3/g is obtained by calculating the area under the CJ isentrope from the CJ pressure to zero pressure. The chemical energy E_o which is used in the computer calculations is obtained from the Hugoniot relation

$$E_{CJ} - E_o = (P_{CJ} + p_o)\ (V_o - V_{CJ})/2. \qquad (9)$$

This gives E_o = 0.0587 megabar-cm^3/g. E_o is the energy which is added to the specific internal energy of a zone as the detonation front reaches the zone (see Sec. III).

* The thermochemical calculations were carried out by H. Hurwitz, using the RUBY computer program[9] which contains the Cowan-Fickett version of the Becker-Kistiakowsky-Wilson equation of state[10]. The modified RDX parameters of Mader[11] were used in the calculations.

V. RESULTS OF CALCULATIONS

The results of the calculations on the flow produced by the detonation of a two-inch cylinder of pentolite explosive are summarized in Figs. 3-12. Figures 3-10 and 12 were processed directly from the computer calculations (excluding the labels and dashed-in rarefaction fronts) on a Stromberg-Carlson SC-4020 Microfilm Recorder.

The cross section (parallel to the central axis) of the detonating cylinder is shown in Figs. 3-6 for different instants of time after initiation. Initiation of the detonation is at t=0. The Lagrangian computation grid is plotted on the cross section. The initial grid (Fig. 3) consists of approximately 4000 mesh points. Additional grid is generated as the detonation progresses down the cylinder. At t = 11.3841 microseconds the computation grid has 9000 mesh points (the top half of the grid shown in Fig. 6). The initial zone size of the solid explosive is 0.0508 x 0.05 cm. Individual zones in the solid explosive and the compressed explosion products cannot be clearly distinguished in the figures because of the inadequate resolution of the scale which was chosen for the plots. In Figs. 4-6, however, the zone configuration is discernible in the region where the gas has undergone some expansion. At 2.9753 microseconds after initiation (Fig. 4), the detonation has not yet reached the side of the cylinder. The detonation-product gas expands only out the end-face of the cylinder. After the detonation reaches the side of the cylinder (Fig. 5) the gas expands radially as well. The cross section at t = 11.3841 microseconds is shown in Fig. 6. The

Lagrangian grid line which was originally the end-face surface of the solid explosive was dropped from the calculations at t = 9.9171 microseconds and therefore does not appear in Fig. 6.

The pressure distribution in the product gas at specific times after initiation is illustrated in Figs. 7-10. Here, the positions of the isobars in the cross section of the detonation are shown. The leftmost isobar is the 10 kilobar line. On each consecutive isobar to the right, the pressure increases by 10 kilobars. The detonation front is at the CJ pressure of 245 kilobars. The head of the rear and lateral rarefaction waves are shown by dashed lines. The head of the lateral rarefaction wave can be located on each isobar ($\geq$ 60 kb) at the point where the isobar departs from being circular. On the central axis, the head of the rear rarefaction wave moves with the 55 kb isobar. In Fig. 7, only the rear rarefaction wave exists. In Figs. 8 and 9, both rarefactions can be seen. The head of the lateral rarefaction impinges on the central axis at t = 11.3841 microseconds (Fig. 10), thereby annihilating the rear rarefaction wave. At subsequent times, the head of the rear rarefaction wave does not appear.

It should be noticed that the flow is entirely spherical in the region (detonation head) bounded by the heads of the rear and lateral rarefaction waves and the detonation surface. Moreover, this spherical flow is exactly that which is described by the similarity solution of G. I. Taylor for a spherical detonation[12] (Hereafter referred to as the spherical Taylor wave). In Fig. 11, the pressure and particle velocity profiles along the central axis in the CYCLONE

calculations (t = 7.6359 microseconds) are compared to the pressure and particle velocity distribution in a spherical Taylor wave.* The two sets of data are shown to be in exact agreement in the region where the Taylor wave particle velocity is greater than zero. The departure of the two data in the Taylor wave region of zero particle velocity is due to the two different boundary conditions at the initiation point. In the Taylor similarity solution the detonation is spherical and the geometry imposes the boundary condition that the gas at the point of initiation remain fixed. In the CYCLONE calculations the detonation is hemispherical and the gas at the point of initiation on the central axis is allowed to expand freely.

The expansion of the gas along the axis causes a rarefaction wave to follow the detonation front. This rear rarefaction wave exists only until it is annihilated by the lateral rarefaction wave impinging on the central axis. Previous to this time, the penetration of the rear rarefaction wave, along the axis, is known since the position of the head of this wave must correspond with the "sonic point" (point of zero particle velocity) in the Taylor wave. We see from Fig. 11 that this is so.

---

* This Taylor wave was numerically generated with the use of W. A. Walker's computer routines[13]. The equation of state for the detonation products given in Sec. IV was used in the Taylor wave calculations.

The effect of the von Neumann-Richtmyer finite difference method on the flow variables at the shock front is demonstrated in Fig. 11. The pressure and particle velocity profiles are "rounded" at the shock front and a small "tail" precedes the actual position of the shock front. This typical characteristic of the numerical method produces an inherent "edge" effect in the calculations. The "tail" causes the unreacted explosive at the cylindrical surface to expand before it is "detonated" by the computer program. Therefore the lateral rarefaction wave proceeds into the cylinder about 0.3 microseconds sooner than it would if the shock-detonation front were infinitely thin.

The specific volume (or density, since $\rho = 1/V$) distribution in the cross section of the detonating cylinder at t=11.3841 microseconds is shown in Fig. 12. The isochore furthest from the detonation front is V=1.50 cm^3/g. The specific volume decreases by 0.05 cm^3/g on each consecutive isochore closer to the detonation front. At the detonation front, the specific volume is $V=1/\rho_{CJ}=1/2.210=0.4525$ cm^3/g. The specific volume distribution in the detonation head region is identical to the specific volume distribution in a spherical Taylor wave.

VI. DISCUSSION

The results of the calculations (Sec. V) are, of course, only valid for that part of the detonation where our physical and mathematical model of the detonation is consistent with the experimental data. More specifically, it is valid over that region where the shape of the detonation front can be represented by an expanding sphere of radius $D_{CJ}t$. From the extensive experimental data of Cook,

et al[1]., this is shown to be for a charge length of 3.5 charge diameters for pentolite, in particular, and for charge lengths of 1 to 4 charge diameters for solid explosives, in general. Since the calculations were carried out to where the detonation front was 1.71 charge diameters from the point of initiation, we are well within the limitations of our model.

In addition to the specific numerical results obtained, more general conclusions can be made. We have shown that the flow immediately behind the detonation front in the region unaffected by the rear and lateral rarefaction wave, is, identically, the Taylor similarity flow for a spherical detonation. Since the characteristic of similarity flows is that the flow variables depend only on their relative position in the flow, we are able to determine the flow in this region for later times. That is, at least to the point where the radius of curvature of the detonation front is equal to 3.5 charge diameters which is the upper limit of our detonation model according to Cook's data. From the rather limited experimental data of Jaffe and Clairmont[4], the indication is that our model of the detonation may hold over a much greater distance. Therefore, perhaps, the Taylor similarity solution may be validly extended to charge lengths greater than 3.5 charge diameters.

It should be pointed out that although one can obtain the flow in the detonation head region for later times because it is a similarity flow, one cannot, however, determine the shape of this region by extrapolating the calculated results. The shape of the detonation head has to be determined by calculating the motion of the lateral rarefaction front into the spherical Taylor wave flow of the detonation head.

VII. ACKNOWLEDGEMENTS

The author is indebted to Dr. H. M. Sternberg for suggesting the problem and providing helpful advice during the course of making the numerical calculations, and to Drs. D. Price and S. Jacobs for taking time for consultations and for their interest in the problem. The author also wishes to thank H. Hurwitz for making the RUBY thermochemical calculations and W. A. Walker for making available his computer routines for generating the Taylor wave.

VIII. REFERENCES

1. M. A. Cook, et al., J. Appl. Phys., 27, 269 (1956).

2. T. Orlow, D. Piacesi, and H. M. Sternberg, Naval Ordnance Laboratory Report NOLTR 7265, (September 1960).

3. Ia. B. Zeldovich and A. S. Kompaneets, Theory of Detonation, (Academic Press, New York and London, 1960).

4. I. Jaffe and A. R. Clairmont, Naval Ordnance Laboratory Report NOLTR 65-33, (June 1965).

5. J. Von Neumann and R. D. Richtmyer, J. Appl. Phys., 21, 232 (1950).

6. J. W. Enig, J. Math. and Phys., Vol XI, No. 1, (April 1961).

7. N. L. Coleburn and T. P. Liddiard, Jr., J. Chem. Phys., 44 1929, (1966).

8. H. M. Sternberg and D. Piacesi, Phys. Fluids, 9, 1307, (1966).

9. H. B. Levine and R. E. Sharples, University of California, Lawrence Radiation Laboratory Report UCRL-6815, (March 1962).

10. R. D. Cowan and W. Fickett, J. Chem. Phys., 24, 932 (1956).

11. C. L. Mader, Los Alamos Scientific Laboratory Report LA-2900, (July 1963).

12. G. I. Taylor, Proc. Roy. Soc., A, 200, 235 (1950).

13. W. A. Walker and H. M. Sternberg, presented at Fourth Symposium on Detonation, (Oct 12-15, 1965), to be published in the proceedings (1967).

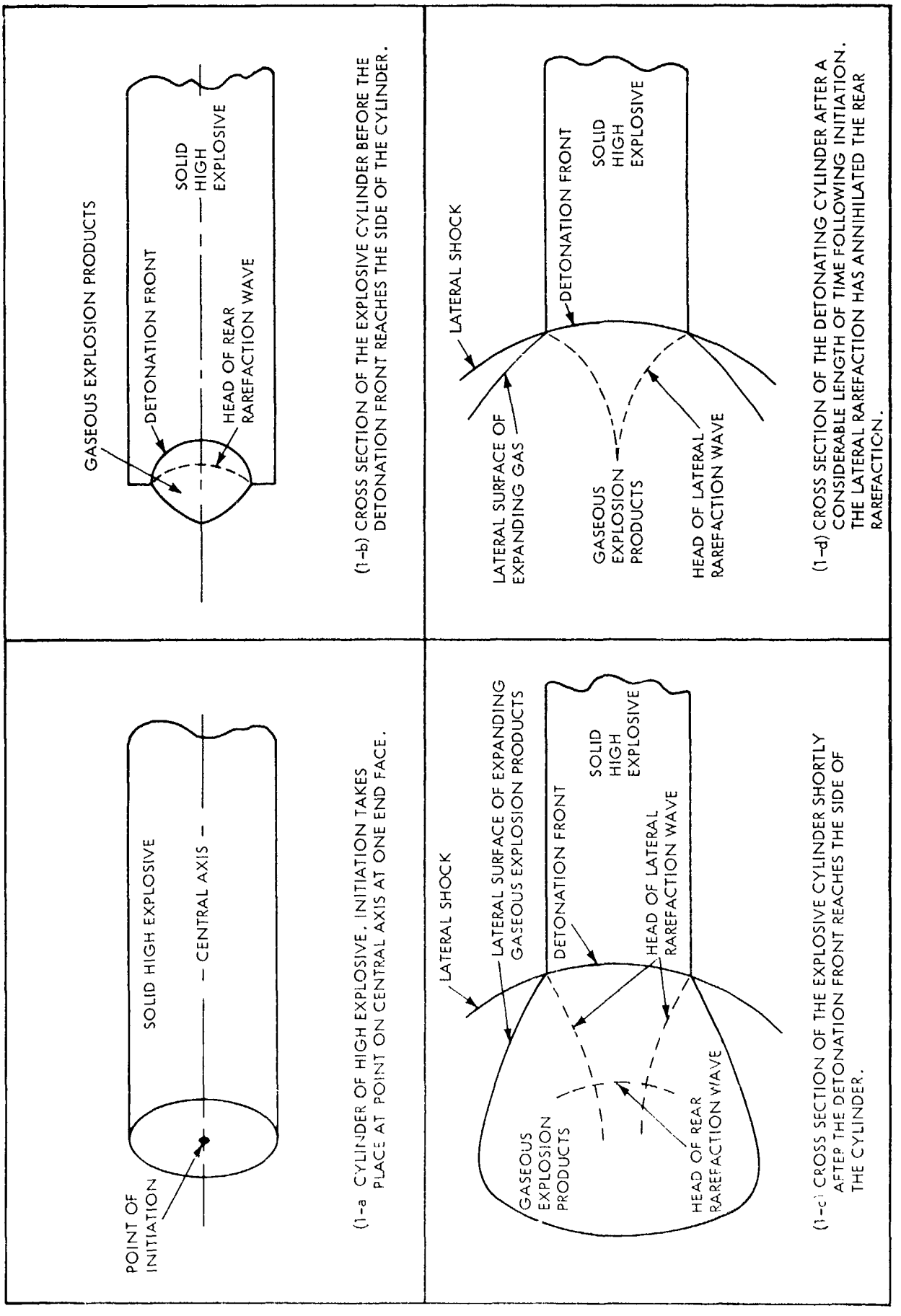

FIG. 1 A QUALITATIVE DESCRIPTION OF THE FLOW IN A POINT-INITIATED CYLINDER OF EXPLOSIVE

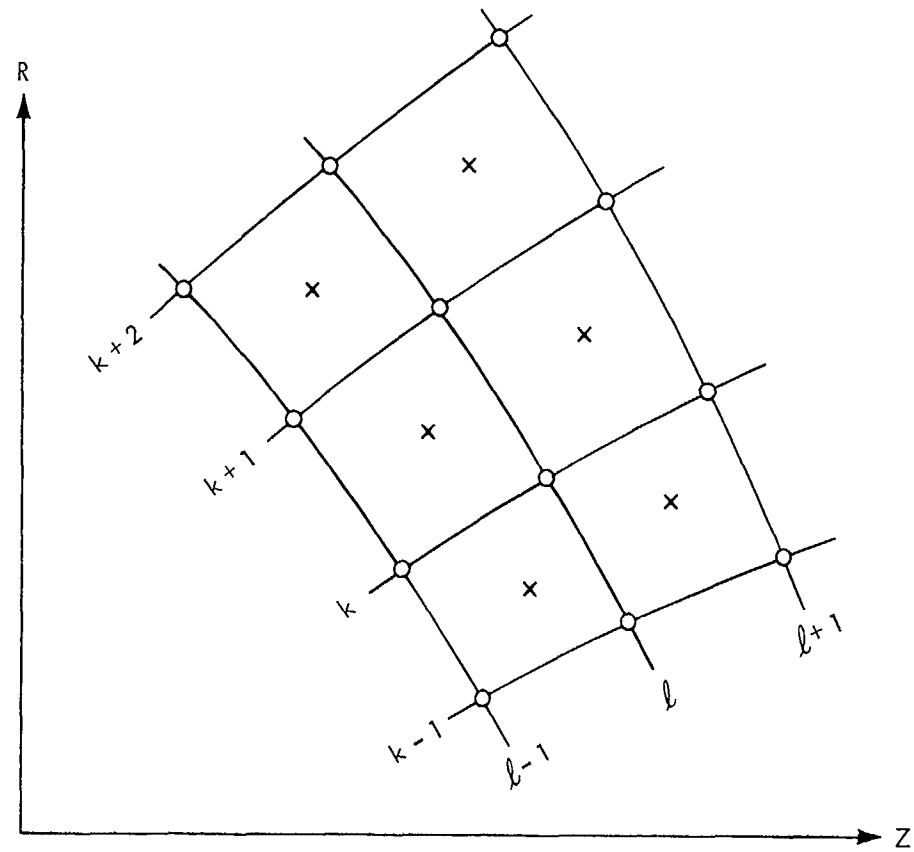

FIG. 2 A GENERAL LAGRANGIAN COMPUTATION GRID. MASS POINTS ARE LOCATED AT THE INTERSECTION OF THE k, ℓ LINES. POSITIONS AND VELOCITIES ARE ASSOCIATED WITH EACH MASS POINT. PRESSURE, SPECIFIC VOLUME, INTERNAL ENERGY, AND AN ARTIFICIAL VISCOSITY ARE LOCATED AT THE CENTER (X's) OF THE QUADRILATERALS ("ZONES").

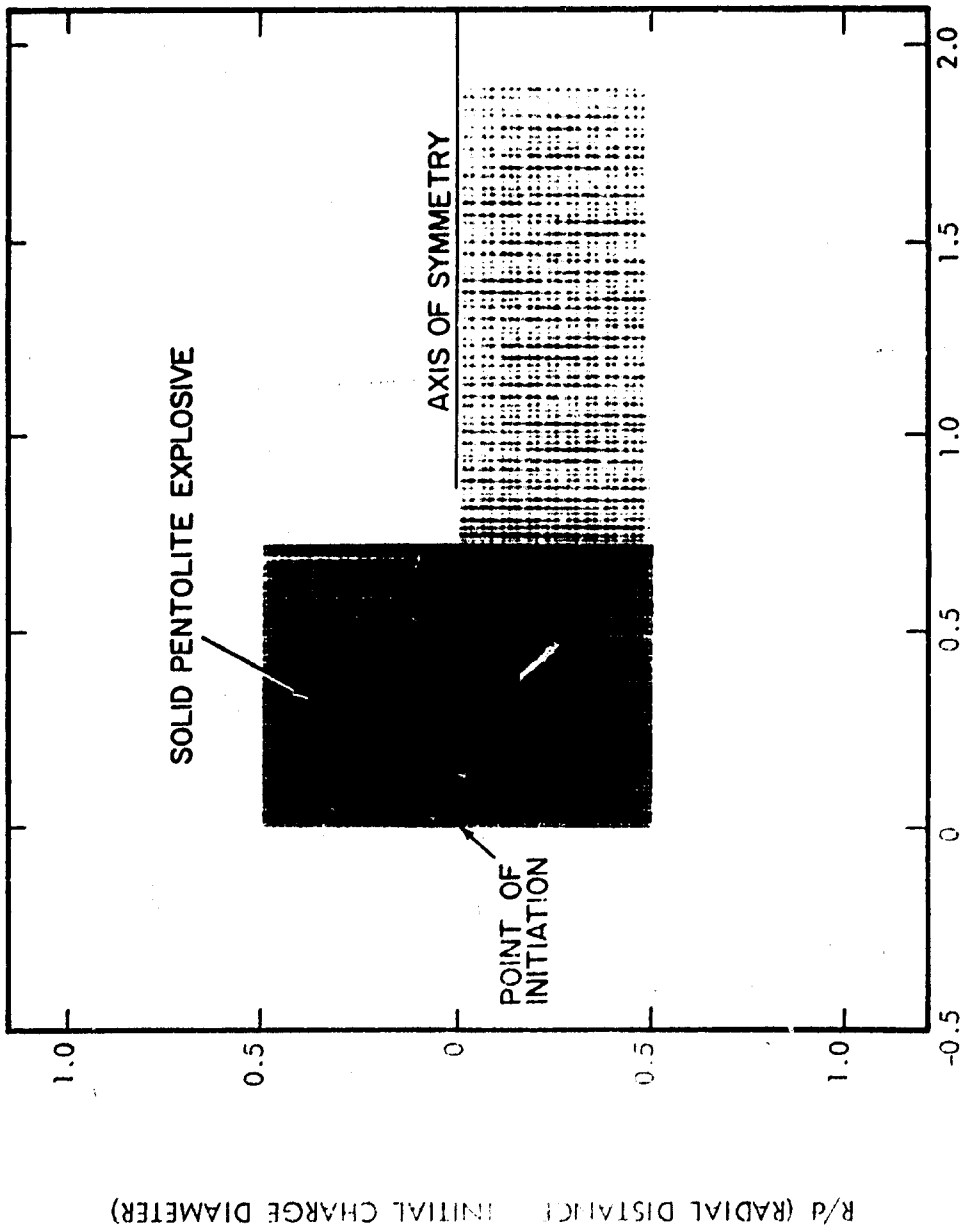

FIG. 3 Cross section of a two inch diameter cylinder of pentolite. The initial Lagrangian computation grid is shown on the cross section. The computations are made with the half of the grid which is above the axis of symmetry. The bottom half of the grid is plotted as the mirror image of the top half. The point of initiation is at (R/d, Z/d) = (0,0).

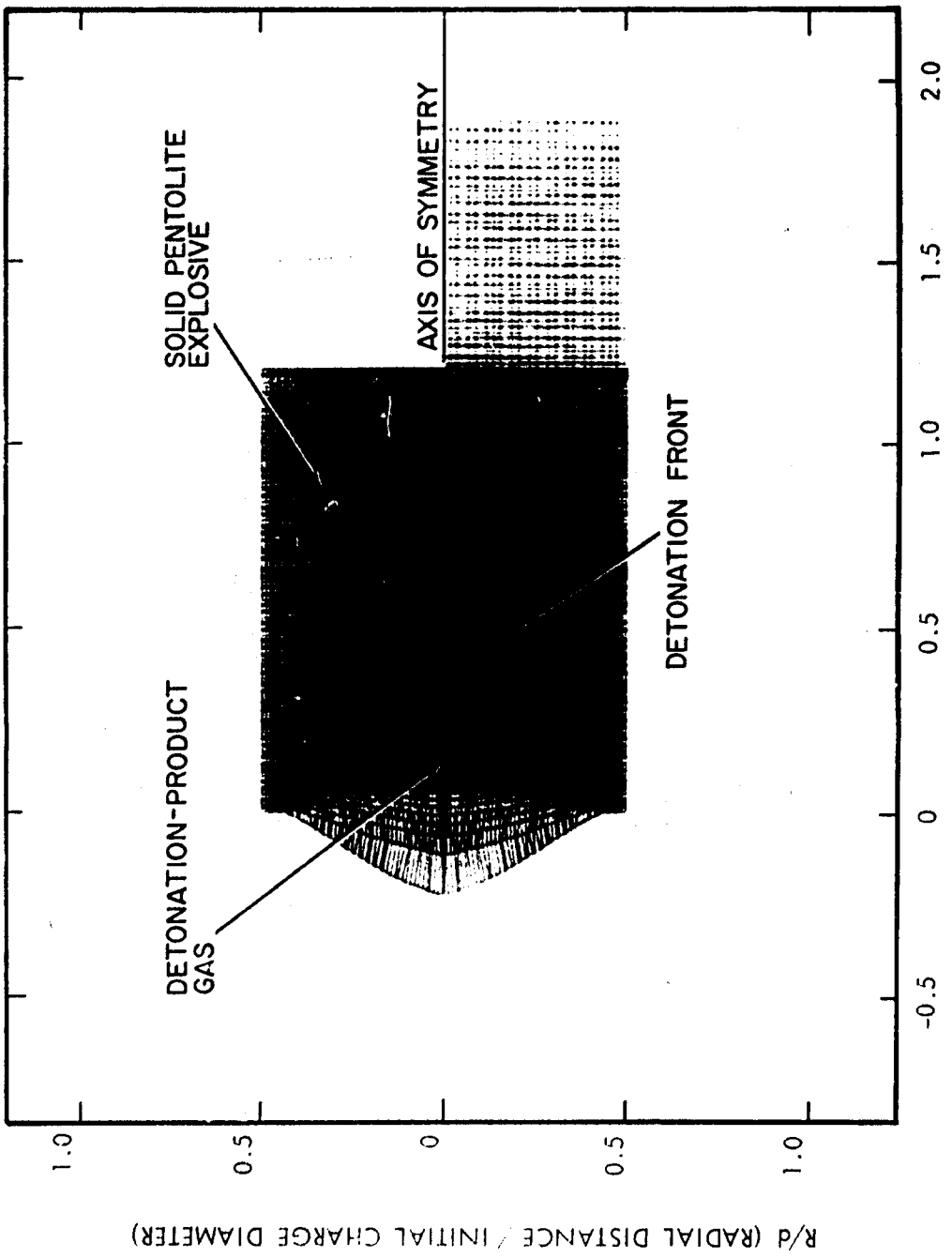

FIG. 4 Cross section of the detonating cylinder at 2.9753 μseconds after initiation. The detonation front has not yet reached the side of the cylinder. Point of initiation is at (R/d, Z/d = (0,0).

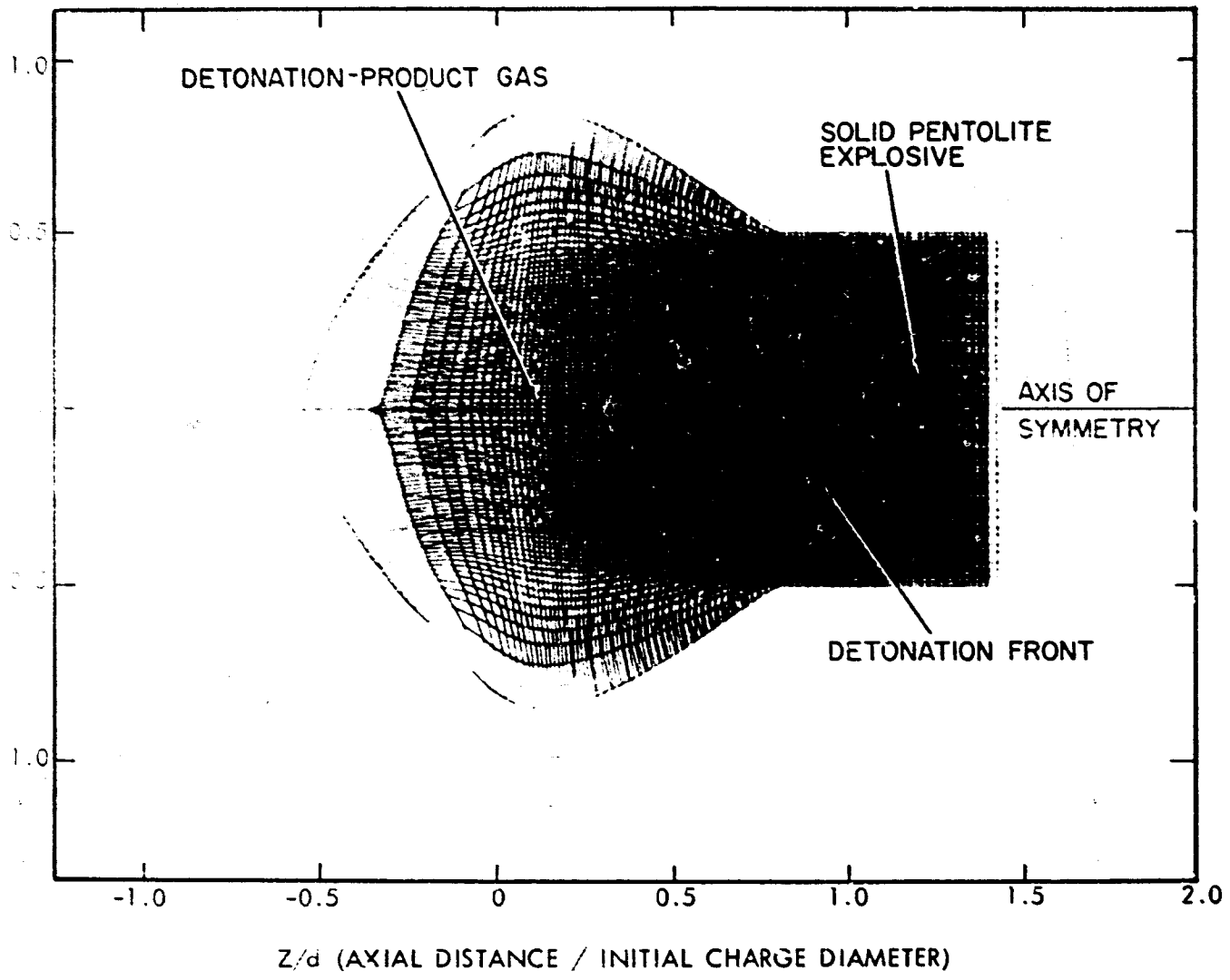

FIG. 5 Cross section of the detonating cylinder at 6.249 μseconds after initiation. The detonation front has reached the side of the cylinder and the detonation-product gas expands radially. Point of initiation is at (R/d, Z/d) = (0, 0).

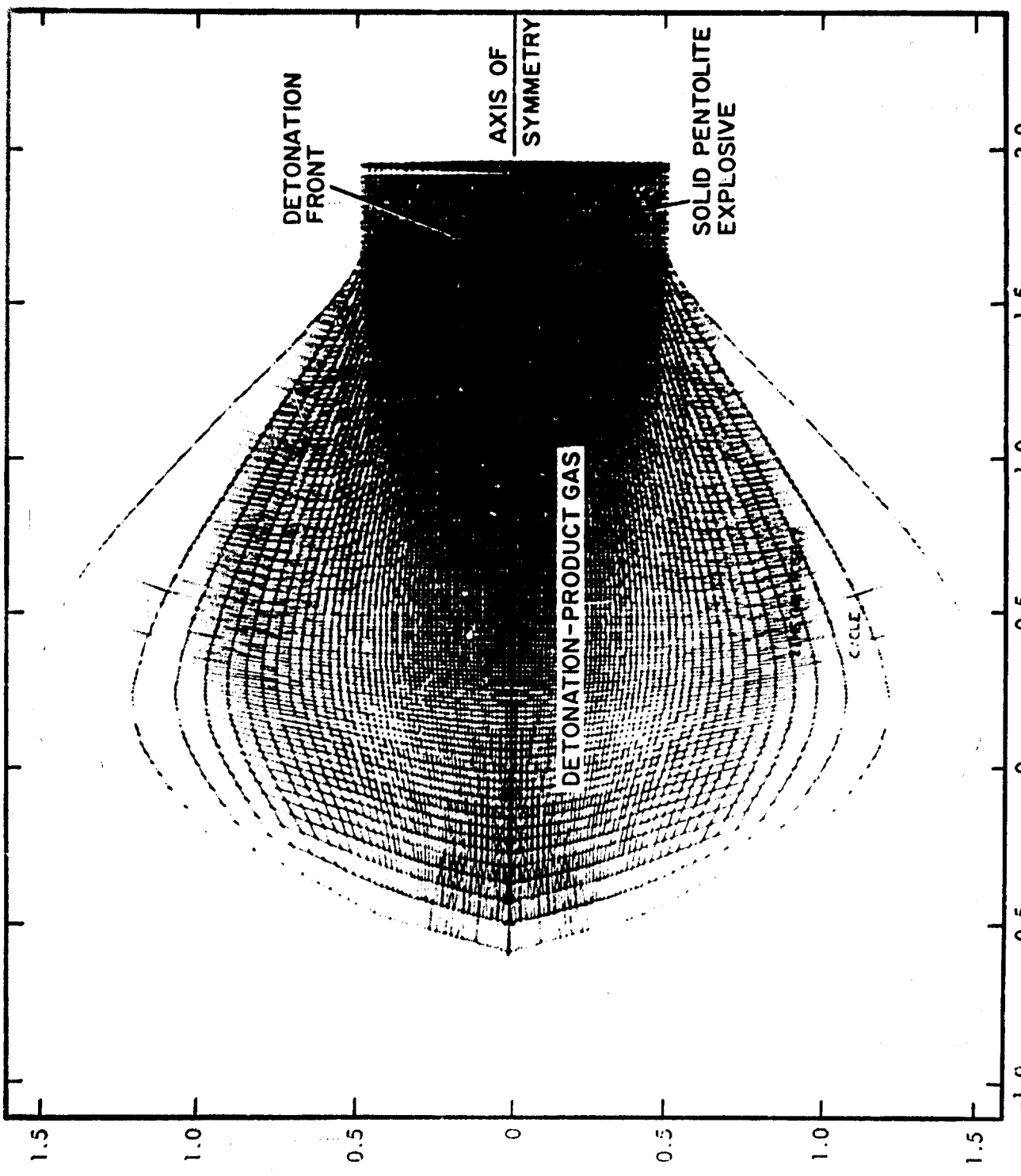

FIG. 6 Cross section of the detonating cylinder at 11.3841 μ seconds after initiation. Point of initiation is at $(R/d, Z/d) = (0,0)$.

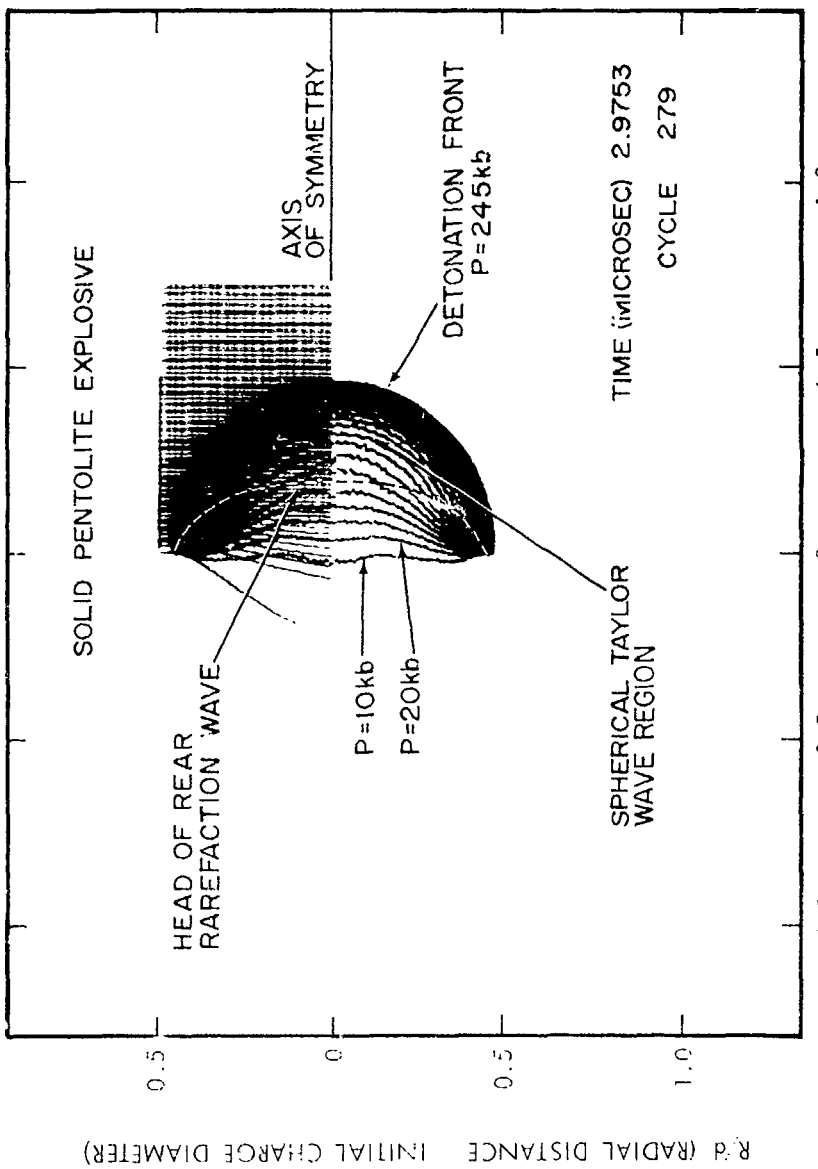

FIG. 7 The pressure distribution in the form of isobars is shown in the cross section of the detonating cylinder at 2.9753 μ seconds after initiation. There is a difference of 10 kilobars between adjacent isobar lines (actually a set of discrete points) with the leftmost isobar = 10kb and the pressure at the detonation front = 245kb. Point of initiation is at (R/d, Z/d) = 0,0.

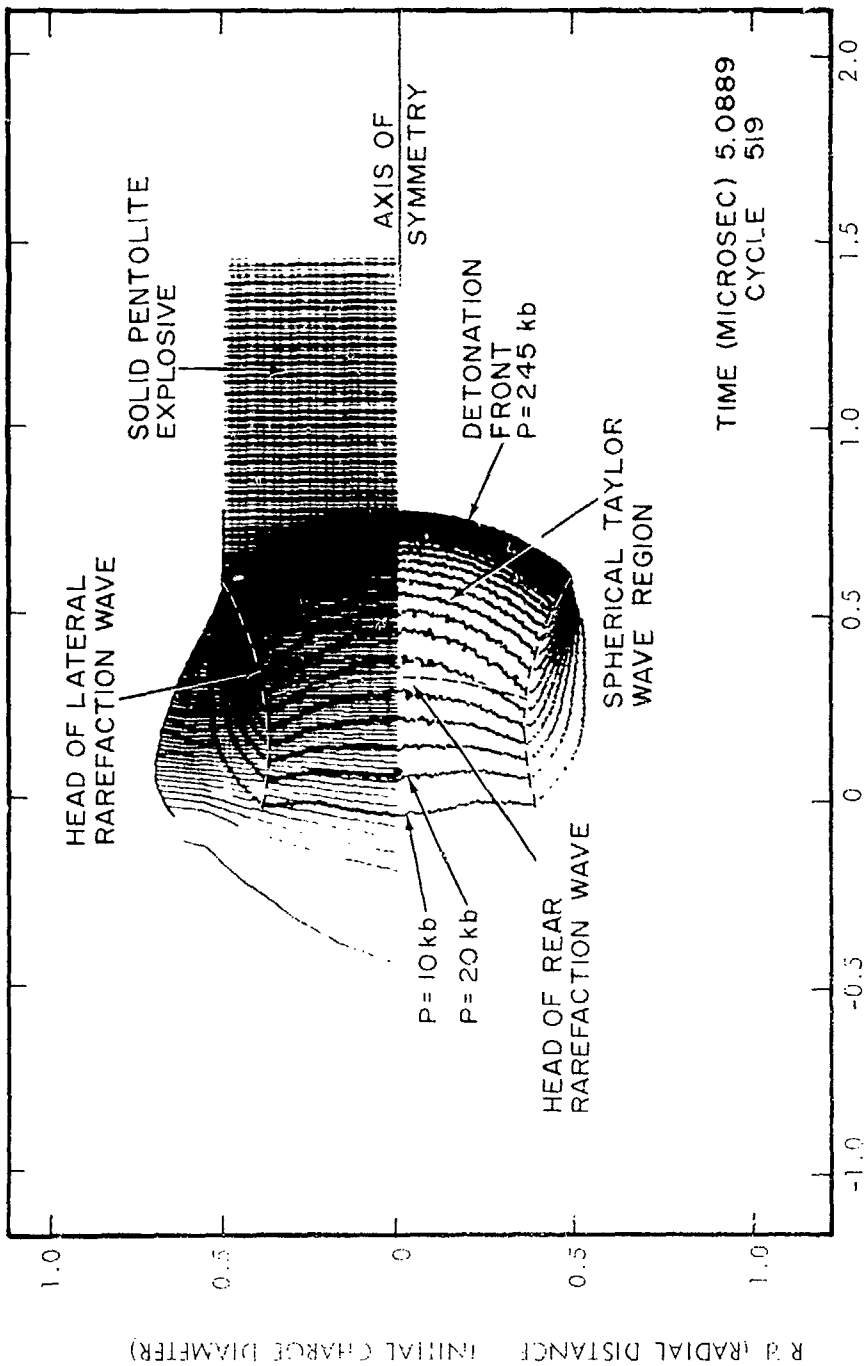

FIG. 8 The pressure distribution in the form of isobars is shown in the cross section of the detonating cylinder at 5.0889 μseconds after initiation. There is a difference of 10kb between adjacent isobar lines. Point of initiation is at $(R/d, Z/d) = (0,0)$.

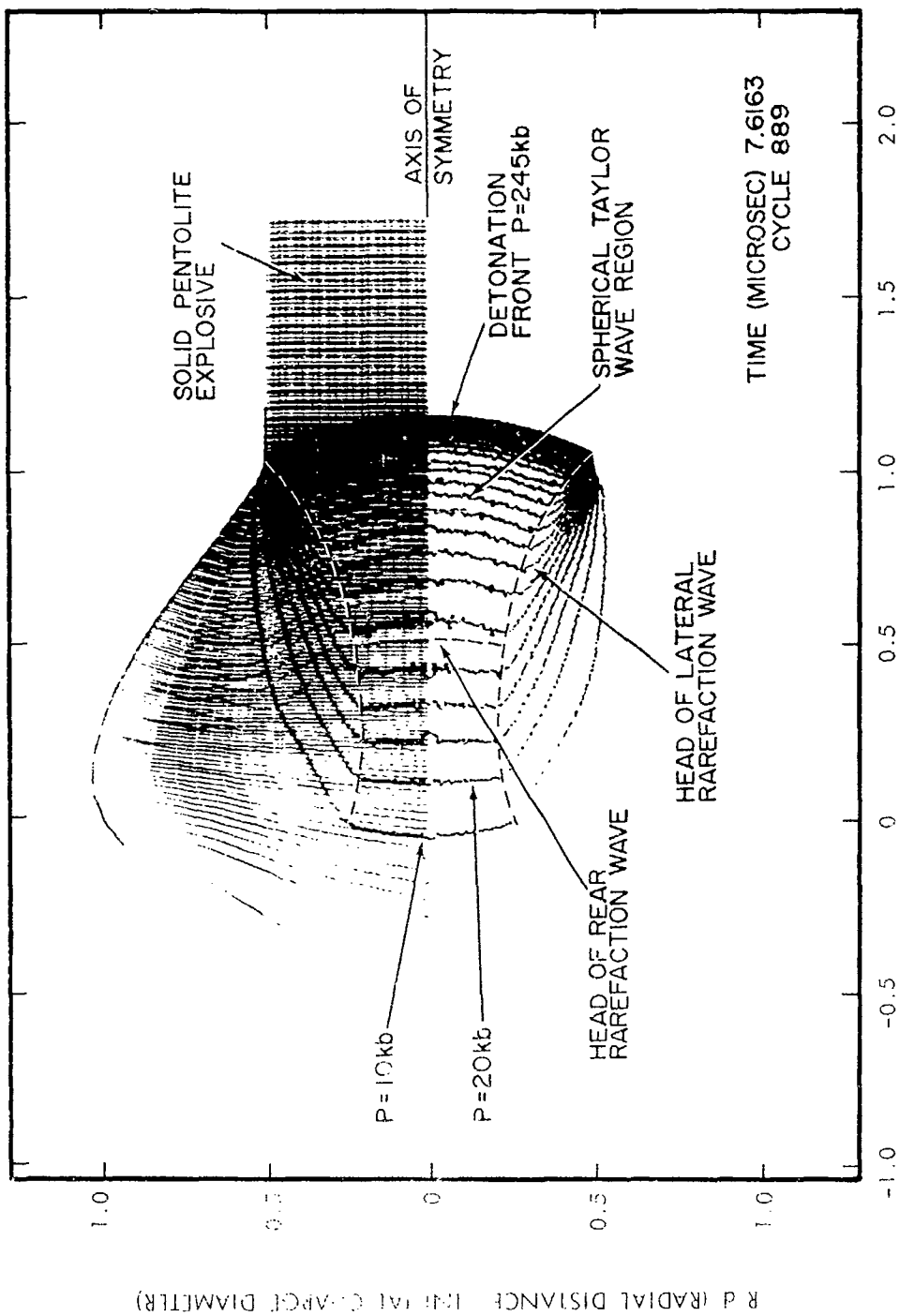

FIG. 9 The pressure distribution in the form of isobars is shown in the cross section of the detonating cylinder at 7.6163 μ seconds after initiation. There is a difference of 10kb between adjacent isobar lines. Point of initiation is at (R/d, Z/d) = (0, 0).

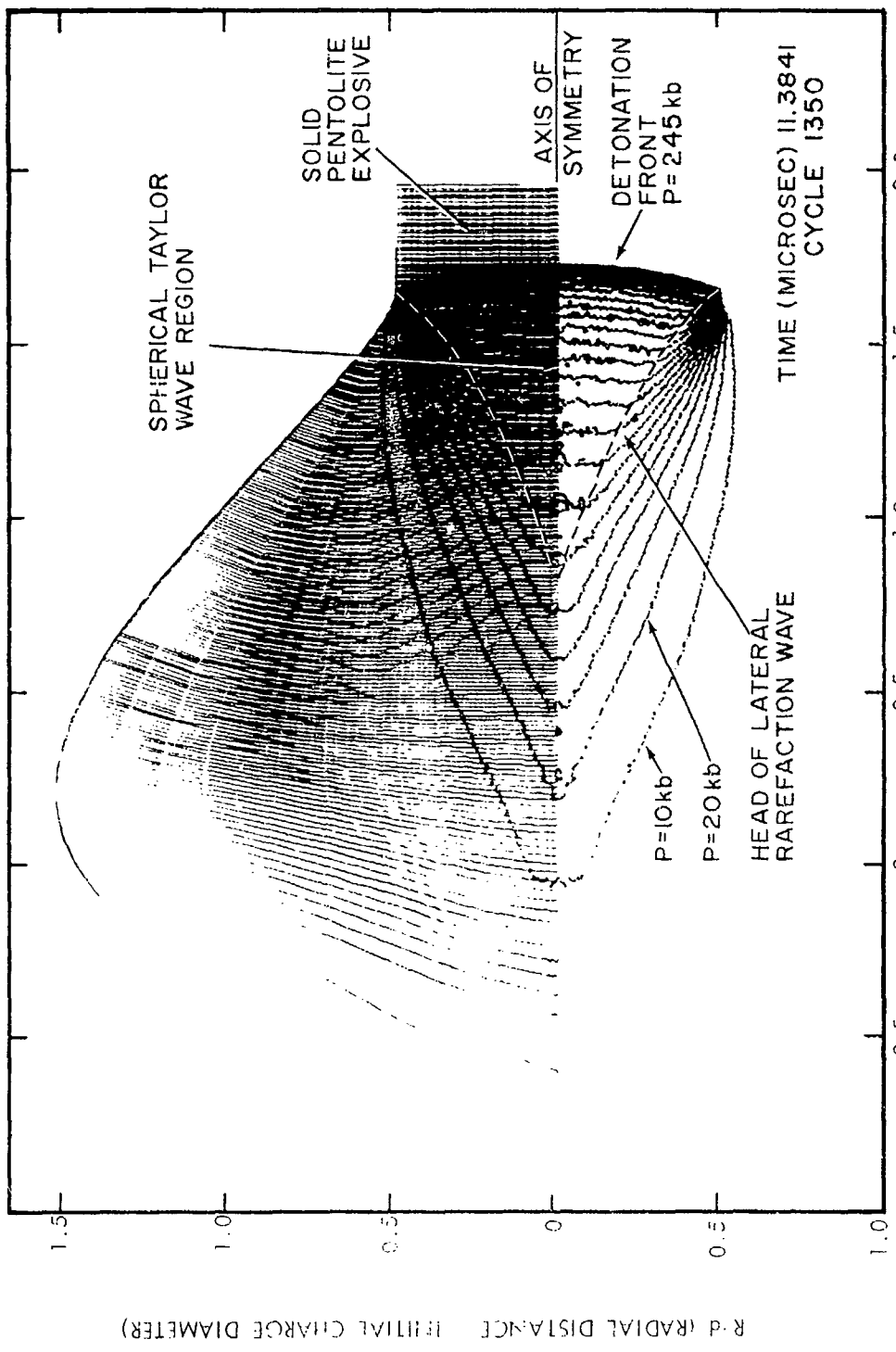

FIG. 10 The pressure distribution in the form of isobars is shown in the cross section of the detonating cylinder at 11.3841 μ seconds after initiation. There is a difference of 10kb between adjacent isobar lines. Point of initiation is at $(R/d, Z/d) = (0,0)$.

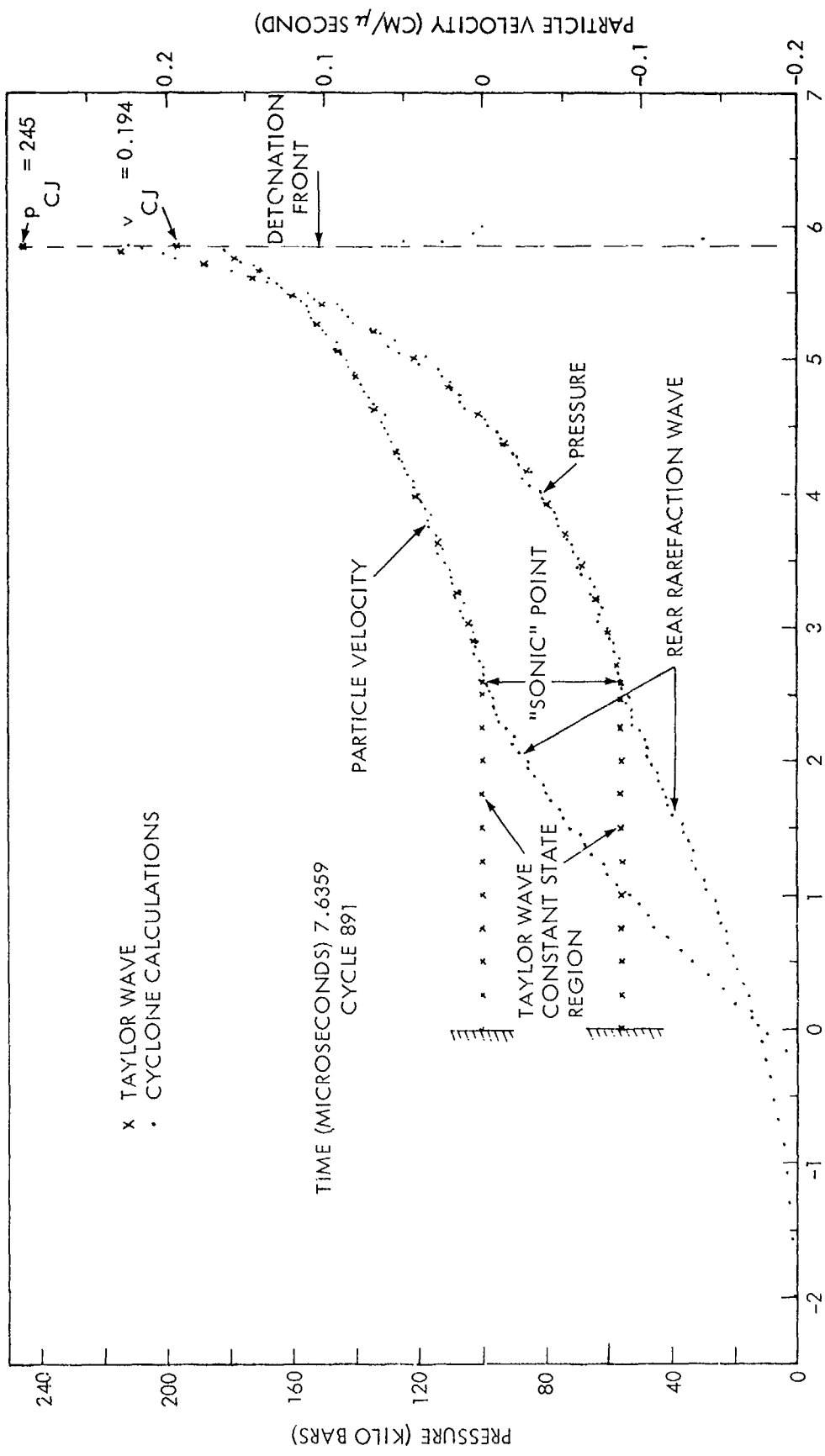

FIG. 11 Comparison of the pressure and particle velocity along the central axis (CYCLONE calculations) and the radial pressure and particle velocity distribution in a spherical Taylor wave. The CYCLONE values are taken at t=7.6359 microseconds after initiation. The Taylor wave was generated with the computer routines which are described in reference (13). Point of initiation is at Z=0.

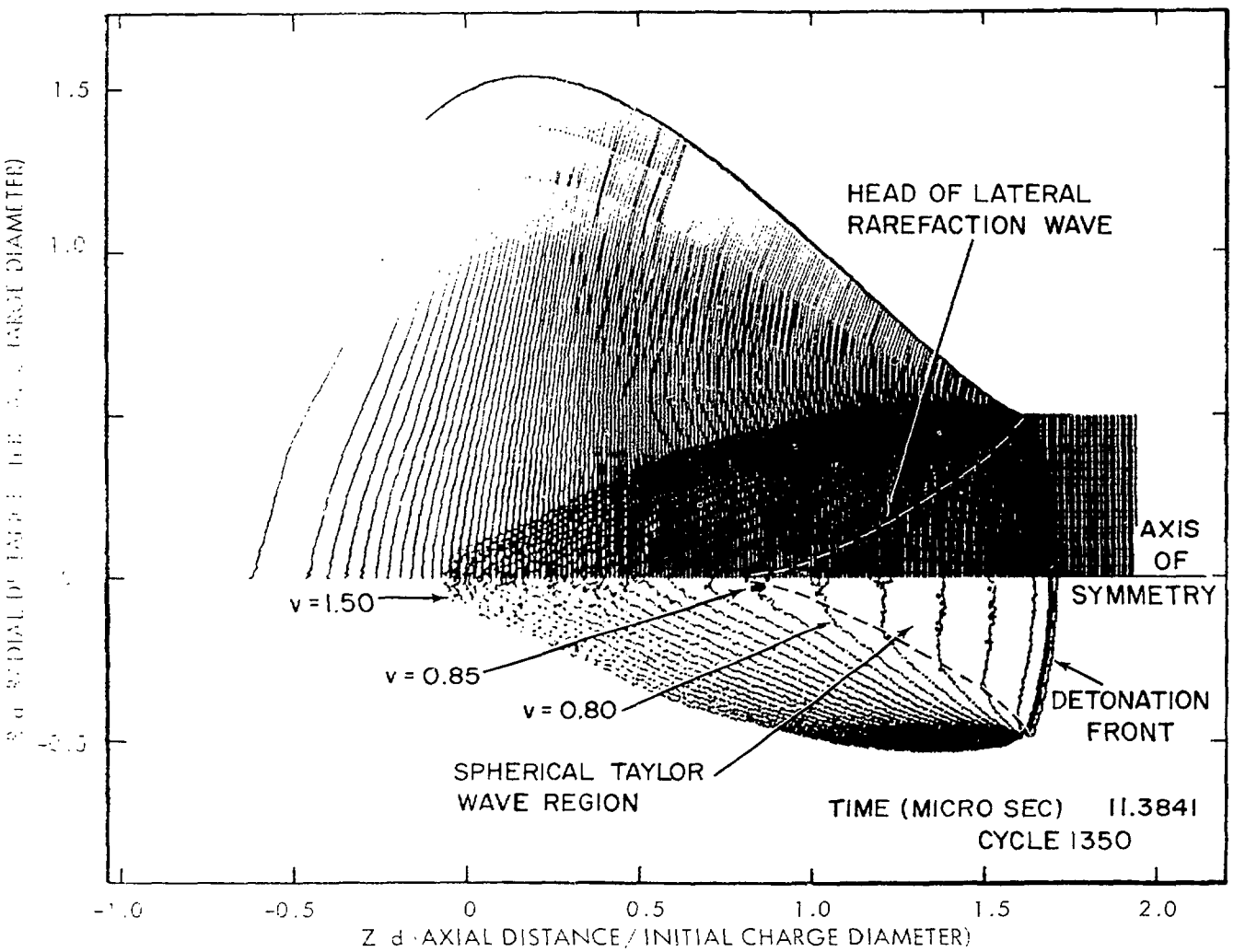

FIG. 12 The specific volume distribution in the cross section of the detonating cylinder at t=11.3841 μ seconds. The isochore furthest from the detonation front is V = 1.50 cm^3/g. The difference between isochores is 0.05cm^3/g. At the detonation front, V = 0.452 cm^3/g. This isochore does not appear in the figure. The three lines at the detonation front (starting from the right V=0.60, 0.55, and 0.50) are a result of the finite difference method which produces a continuous transition of the flow variables across the shock.

DISTRIBUTION

	Copies
Technical Library **U. S. Naval** Ordnance Station Indian Head, Maryland 20640	1
Commanding Officer Naval Weapons Station (ORR) Yorktown, Virginia 23491	1
Commanding Officer & Director David Taylor Model Basin Washington, D. C. 20007 Attn: Central Library Branch, Code 042-043	1
Commander U. S. Naval Weapons Laboratory Dahlgren, Virginia 22448 Technical Library J. Talley D. Abernathy Terminal Ballistics Laboratory	1 1 1 1
Underwater Explosions Research Division David Taylor Model Basin Portsmouth, Virginia 23709	1
Commanding Officer U. S. Army Ballistic Research Laboratories Aberdeen Proving Ground, Md. 21005 Attn: AMXBR-XS Dr. R. Eichelberger	1 1
Director Applied Physics Laboratory Johns Hopkins University 8621 Georgia Avenue Silver Spring, Maryland 20910 Attn: Document Librarian L. Welanetz M. Friedman	1 1 1
R. Stresau Laboratory, Inc. Star Route Spooner, Wisconsin 54801	1
APGC (PGBPS-12) Eglin AFB, Florida 32542 Attn: Virginia B. Harvey	1

	Copies
Commander Naval Air Systems Command Washington, D. C. 20360 AIR-604	1
Commanding General Frankford Arsenal Philadelphia, Pennsylvania 19137 Attn: C2500, Library	1
Research Director, Explosives Research Center Bureau of Mines 4800 Forbes Avenue Pittsburgh, Pa., 15213 Attn: R. W. Van Dolah	1
Systems Engr. Group (R&T) Wright Patterson AFB, Ohio 45433 SEPIR	1
Sandia Corporation P. O. Box 969 Livermore, California 94550 Attn: Document Control	1
Commanding General U. S. Army Missile Command Redstone Arsenal, Alabama 35809 Attn: Technical Library	1
Sandia Corporation P. O. Box 5800 Albuquerque, New Mexico 87115 Attn: Technical Library	1
Commanding Officer U. S. Naval Ordnance Laboratory Corona, California 91720 Library Division	1
Commanding Officer Naval Underwater Weapons Research and Engineering Station Newport, Rhode Island 02840	1
Commanding Officer U. S. Naval Ammunition Depot Crane, Indiana 47522 QEL	1

	Copies
Commander U. S. Naval Ordnance Test Station China Lake, California 93555	
Technical Library (Code 753)	1
Dr. C. D. Lind	1
Superintendent Naval Post Graduate School Monterey, California 93940	
Code 2124	1
Lockheed Missile & Space Corporation (LMSC) 599 S. Mathilda Dept. 27-11 Sunnyvale, California 94086	1
Stanford Research Institute Polymer and Propulsion Sciences Div. Menlo Park, California 94025	1
Commanding Officer U. S. Naval Weapons Evaluation Facility Kirtland Air Force Base Albuquerque, New Mexico 87117	1
Commanding Officer Harry Diamond Laboratories Connecticut Ave., & Van Ness Streets, N. W. Washington, D. C. 20438	
Library	1
Defense Documentation Center Cameron Station Alexandria, Virginia 22314	20
Space Ordnance Systems, Inc. 122 Penn Street El Segundo, California 90246	
Dell Lytle	1
Director Naval Research Laboratory Washington, D. C. 20390	
Code 2027	1
NASA Scientific and Technical Information Facility P. O. Box 33 College Park, Maryland 20740	1

	Copies
Commanding Officer Picatinny Arsenal Dover, New Jersey 07801	
SMUPA-G	1
SMUPA-VA6	1
SMUPA-DD	1
SMUPA-DR4	1
SMUPA-DW	1
SMUPA-VC	1
SMUPA-VE	1
SMUPA-VL	1
SMUPA-TX	1
SMUPA-TW	1
SMUPA-W	1
SMUPA-DR	1
Army Materiel Command Department of the Army Washington, D. C. 20315	
R&D Division	1
NASA Goddard Space Flight Center Greenbelt, Maryland 20771	1
Director Los Alamos Scientific Laboratory P. O. Box 1663 Los Alamos, New Mexico 87544	
Attn: Report Librarian	1
Aerojet-General Corporation Research Division 11711 Woodruff Avenue Downey, California	
Attn: Dr. H. J. Fisher	1
Hercules Incorporated Allegany Ballistics Laboratory P. O. Box 210 Cumberland, Maryland 21502	
Attn: Technical Library	1
The Martin Company Herndon Airport 815 Elwell Street Orlando, Florida 32800	
J. Allred	1

	Copies
Commanding General Air Force Systems Command Andrews Air Force Base Camp Springs, Maryland 20331	1
The Boeing Company Aero-Space Division P. O. Box 3707 Seattle, Washington 98124 Applied Math. Info. Center	1
New Mexico Institute of Mining & Technology Campus Station Socorro, New Mexico M. E. Hanson	1
Stanford University Department of Aeronautical Engineering Stanford, California 94305	1
The University of Texas Defense Research Laboratory P. O. Box 8029 Austin, Texas 78712	1
University of Washington Department of Aeronautical Engineering Seattle, Washington, 98122	1
Yale University Department of Chemistry New Haven, Connecticut Dr. John P. Chesick	1
Institute for Cooperative Research Johns Hopkins University 1315 St. Paul Street Baltimore, Maryland 21202	1
University of Missouri at Rolla Rock Mechanics Research Group Rolla, Missouri 65401 Dr. R. Rollins	1

	Copies
Shock Hydrodynamics, Inc. Sherman Oaks, California 91403 Dr. L. Zernow	1
Commander Naval Air Development Center Johnsville, Pennsylvania 18974 Attn: Aviation Armament Laboratory	1
Commanding Officer Office of Ordnance Research Box CM Duke Station Durham, North Carolina 27706	1
Commanding Officer Engineer Research & Development Laboratory Ft. Belvoir, Virginia 22060 Technical Intelligence Branch	1
Commanding Officer U. S. Naval Weapons Evaluation Facility Kirtland Air Force Base Albuquerque, New Mexico 87117	1
Director Lewis Research Center National Aeronautics & Space Administration 21000 Brookpark Road Cleveland, Ohio 44135	1
NASA Langley Research Center Hampton, Virginia 23365 Attn: Mr. C. Breen	1
U. S. Atomic Energy Commission Technical Information Extension P. O. Box 62 Oak Ridge, Tennessee 37830	1
U. S. Atomic Energy Commission Washington, D. C. 20545 DMA	1
University of California Lawrence Radiation Laboratory Livermore, California 94550 Attn: M. Wilkins	1

	Copies
Aeronautical Engineering Review 2 East 64th Street New York, New York 14304	1
Mechanics Research Department American Machine and Foundry Co. 188 W. Randolph Street Chicago, Illinois 60601	1
ITT Research Institute 10 West 35th Street Chicago, Illinois 66616 Attn: J. Kennedy	1
Atlantic Research Corporation Alexandria, Virginia 22304 Attn: Dr. A. Macek	1
AVCO-Everett Research Laboratory 2385 Revere Beach Parkway Everett, Massachusetts 02149	1
AVCO-Manufacturing Company 155 Sniffins Lane Stratford, Connecticut 06947	1
AVCO-Manufacturing Company Research & Advanced Development Division 20 South Union Street Lawrence, Massachusetts 01843 Chief, Technical Library	1
AVCO Research Laboratory 2385 Revere Beach Parkway Everett, Massachusetts 02149	1
Bell Aircraft Corporation P. O. Box 1 Buffalo, New York 14201 Attn: Library	1
Boeing Airplane Company Box 3107 Seattle, Washington 98114	1
CONVAIR P. O. Box 1011 Pomona, California 91769 Attn: Library	1

Copies

Douglas Aircraft Company, Inc;
827 Lapham Street
El Segundo, California 90245
Attn: Library 1

Cornell Aeronautical Lab., Inc.
4455 Gennessee Street
Buffalo, New York 14225
Attn: Library 1

Fairchild Engine and Aircraft Co.
Guided Missiles Division
Wyandanch, L. I., New York 11798
Attn: Library 1

General Applied Science Lab., Inc.
Meadowbrook National Bank Building
60 Hempstead Avenue
Hempstead, New York 11552 1

General Electric Company
Aeroscience Laboratory - MSVD
3750 D Street
Philadelphia, Pennsylvania 19124
Attn: Dr. H. Lew 1

General Electric Company
Research Laboratory
P. O. Box 1088
Schenectady, New York 12301
Attn: Clarence Vogler 1

Grumman Aircraft Engineering Corporation
Bethpage, L. I., New York 11714
Attn: Library 1

Hughs Aircraft Company
Research and Development Laboratories
Culver City, California 90230
Attn: Library 1

North American Aviation, Inc.
Aerophysics Department
12214 Lakewood Blvd.
Downey, California 90241 1

Plasmadyne
3839 S. Main Street
Santa Ana, California 92707
Attn: Dr. R. Waniek 1

	Copies
Radio Corporation of America Princeton, New Jersey 08540	1
Rand Corporation 1700 Main Street Santa Monica, California 90401	1
RIAS, Inc. 7212 Bellona Avenue Baltimore, Maryland 21212 Attn: Library	1
Rocketdyne Canoga Park, California 91303	1
Rohm and Haas Company Redstone Arsenal Research Division Huntsville, Alabama 35801	1
United Aircraft Corporation Research Department 400 Main Street East Hartford, Connecticut 06118 Attn: Library	1
Vitro Laboratories East Orange, New Jersey 07019	1
Vitro Laboratories West Orange Laboratory 200 Pleasant Valley Way West Orange, New Jersey 07052	1
Brown University Division of Engineering Providence, Rhode Island 02912 Attn: Library	1
University of California Engineering Department Los Angeles, California 90024	1
California Institute of Technology Guggenheim Aeronautical Laboratory Pasadena, California 91109	1
California Institute of Technology Jet Propulsion Laboratory 4800 Oak Grove Drive Pasadena, California 91107	1

	Copies
Carnegie Institute of Technology Shenley Park Pittsburgh, Pennsylvania 15213 Attn: Dr. E. M. Pugh	1
Catholic University of America Aeronautical Mechanical Engineering Washington, D. C. 20017 Attn: Library	1
Institute for Air Weapons Research University of Chicago Chicago, Illinois 60637	1
Denver Research Institute University of Denver Denver, Colorado 80210	1
Department of Civil Engineering and Engineering Mechanics Columbia University New York, New York 10027	1
Cornell University Graduate School of Aeronautical Engineering Ithaca, New York 14850	1
College of Engineering Drexel Institute of Technology Philadelphia, Pennsylvania 19104	1
University of Florida Engineering Mechanics Department Gainesville, Florida 32601 Attn: Library	1
Georgia Institute of Technology Department of Mechanical Engineering Atlanta, Georgia 30332 Attn: Library	1
Harvard University Cambridge, Massachusetts 02138 Department of Engineering Sciences Department of Applied Physics	1 1
University of Illinois Urbana, Illinois 61801 Dept. of Theoretical & Applied Mechanics	1

	Copies
University of Maryland College Park, Maryland 20742	
Inst. for Fluid Dyn. and Applied Math	1
Engineering Library	1
Massachusetts Institute of Technology Fluid Dynamics Research Group Cambridge, Massachusetts 02139	1
Naval Supersonic Laboratory Massachusetts Institute of Technology Cambridge, Massachusetts 02139	1
University of Minnesota Rosemount Research Center Rosemount, Minnesota 55068	1
University of North Carolina Physics Department Chapel Hill, North Carolina 27514	1
North Carolina State College Division of Engineering Research Raleigh, North Carolina 27067	
Technical Library	1
Ohio State University Columbus, Ohio 43210	
Attn: Library	1
Aerodynamics Laboratory Polytechnic Institute of Brooklyn 527 Atlantic Avenue Freeport, New York 11520	1
Rensselaer Polytechnic Institute Department of Aero. Engineering Troy, New York 12180	
Attn: Library	1
University of Southern California Engineering Center 3518 University Avenue Los Angeles, California 90007	1
Director U. S. Army Research & Development Laboratory Ft. Belvoir, Virginia 22060	
Chief, Tech. Support Branch	1

	Copies
Director USAF Project Rand VIA. U.S. Air Force Liaison Office The Rand Corporation 1700 Main Street Santa Monica, California 90400	1
U. S. Documents Officer Office of the U. S. National Military Representative, SHAPE APO 55 New York, New York 10000	1
Director Defense Atomic Support Agency Washington, D. C. 20301 J. Moulton	1
U. S. Research Services 1811 Trousdale Drive Burlingame, California 94010	1
President Kaman Nuclear Colorado Springs, Colorado 80900 Attn: Dr. F. Shelton	1
Institute for the Study of Rate Processes University of Utah Salt Lake City, Utah 84112 Attn: Dr. M. A. Cook	1
Director Physics International Co. 2229 4th Street Berkeley, California 94700 Attn: Dr. C. Godfrey	1
Science Communication, Inc. 1079 Wisconsin Avenue, N. W. Washington, D. C. 20007 Attn: Mr. D. O. Myatt	1
Astrophysics Research Corporation 10889 Wilshire Blvd. Los Angeles, California 94700 Attn: Dr. A. Reifman	1

	Copies
Philco Corporation Aeronutronic Division & Philco Research Ford Road Newport Beach, California 92660	1
Houston Research Institute, Inc. 5417 Crawford Street Houston, Texas 77004 Mr. Clark Goodman	1
Forrestal Research Center Library Aeronautical Sciences Bldg. Princeton University Princeton, New Jersey 08540 Librarian	1
Space Sciences Laboratory General Electric Company P. O. Box 8555 Philadelphia, Pennsylvania 19101 Dr. S. M. Scala	1
Falcon Research and Development 1441 Ogden Street Denver, Colorado 80218 Mr. Daniel K. Parks Mr. C. E. Eppinger	1 1
United Electrodynamics P. O. Box 1650 Pasadena, California Mr. O. K. Kowallis	1
Southwest Research Institute 8500 Culebra Road San Antonio, Texas 78206 Dr. W. H. Chu	1
Office of Chief of Naval Operations Operations Evaluation Group Washington, D. C. 20350	1
NASA Scientific & Technical Information Facility P. O. Box 5700 Bethesda, Maryland 20546	1

UNCLASSIFIED

Security Classification

DOCUMENT CONTROL DATA - R & D

Security classification of title, body of abstract and indexing annotation must be entered when the overall report is classified)

1. ORIGINATING ACTIVITY *(Corporate author)*

U. S. Naval Ordnance
White Oak, Silver Spring, Maryland

2a. REPORT SECURITY CLASSIFICATION

UNCLASSIFIED

2b. GROUP

3. REPORT TITLE

NUMERICAL HYDRODYNAMIC CALCULATIONS OF THE FLOW OF THE DETONATION PRODUCTS FROM A POINT-INITIATED EXPLOSIVE CYLINDER

4. DESCRIPTIVE NOTES *(Type of report and inclusive dates)*

5. AUTHOR(S) *(First name, middle initial, last name)*

DANTE PIACESI, Jr.

6. REPORT DATE	7a. TOTAL NO. OF PAGES	7b. NO. OF REFS
13 January 1967	27	13

8a. CONTRACT OR GRANT NO.	9a. ORIGINATOR'S REPORT NUMBER(S)
b. PROJECT NO. ORD-033-221/092-1/F008-08-11 P.A.004	NOLTR 66-150
c.	9b. OTHER REPORT NO(S) *(Any other numbers that may be assigned this report)*
d.	

10. DISTRIBUTION STATEMENT

This document is subject to special export controls and each transmittal to foreign governments may be made only with prior approval of NOL.

11. SUPPLEMENTARY NOTES	12. SPONSORING MILITARY ACTIVITY
	Naval Ordnance Systems Command

13. ABSTRACT

With the use of the NOL two-dimensional hydrodynamics computer program (CYCLONE), a detailed numerical analysis is made of the flow in the product gas of a detonating cylinder of pentolite (50/50 PETN/TNT) explosive. The explosive cylinder is initiated at a point on the central charge axis at one end-face.

DD FORM 1 NOV 65 1473 (PAGE 1)

S/N 0101-807-6801

UNCLASSIFIED

Security Classification

14 KEY WORDS	LINK A		LINK B		LINK C	
	ROLE	WT	ROLE	WT	ROLE	WT
Explosive Hydrodynamics Cylinder Two-dimensional flow						

Naval Ordnance Laboratory, White Oak, Md.
(NOL technical report 66-150)
NUMERICAL HYDRODYNAMIC CALCULATIONS OF THE FLOW OF THE DETONATION PRODUCTS FROM A POINT-INITIATED EXPLOSIVE CYLINDER, by D. Piacesi, jr. 13 Jan. 1967. 27p. charts, tables. NOSC task ORD-033-221/092-1/F008-08-11.
UNCLASSIFIED

With the use of the NOL two-dimensional hydrodynamics computer program (Cyclone), a detailed numerical analysis is made of the flow in the product gas of a detonating cylinder of pentolite (50/50 PETN/TNT) explosive. The explosive cylinder is initiated at a point on the central charge axis at one end-face.

1. Explosives - Hydrodynamics
2. Explosives - Detonation
I. Title
II. Piacesi, Dante, jr.
III. Project

Abstract card is unclassified.

Naval Ordnance Laboratory, White Oak, Md.
(NOL technical report 66-150)
NUMERICAL HYDRODYNAMIC CALCULATIONS OF THE FLOW OF THE DETONATION PRODUCTS FROM A POINT-INITIATED EXPLOSIVE CYLINDER, by D. Piacesi, jr. 13 Jan. 1967. 27p. charts, tables. NOSC task ORD-033-221/092-1/F008-08-11.
UNCLASSIFIED

With the use of the NOL two-dimensional hydrodynamics computer program (Cyclone), a detailed numerical analysis is made of the flow in the product gas of a detonating cylinder of pentolite (50/50 PETN/TNT) explosive. The explosive cylinder is initiated at a point on the central charge axis at one end-face.

1. Explosives - Hydrodynamics
2. Explosives - Detonation
I. Title
II. Piacesi, Dante, jr.
III. Project

Abstract card is unclassified.

Naval Ordnance Laboratory, White Oak, Md.
(NOL technical report 66-150)
NUMERICAL HYDRODYNAMIC CALCULATIONS OF THE FLOW OF THE DETONATION PRODUCTS FROM A POINT-INITIATED EXPLOSIVE CYLINDER, by D. Piacesi, jr. 13 Jan. 1967. 27p. charts, tables. NOSC task ORD-033-221/092-1/F008-08-11.
UNCLASSIFIED

With the use of the NOL two-dimensional hydrodynamics computer program (Cyclone), a detailed numerical analysis is made of the flow in the product gas of a detonating cylinder of pentolite (50/50 PETN/TNT) explosive. The explosive cylinder is initiated at a point on the central charge axis at one end-face.

1. Explosives - Hydrodynamics
2. Explosives - Detonation
I. Title
II. Piacesi, Dante, jr.
III. Project

Abstract card is unclassified.

Naval Ordnance Laboratory, White Oak, Md.
(NOL technical report 66-150)
NUMERICAL HYDRODYNAMIC CALCULATIONS OF THE FLOW OF THE DETONATION PRODUCTS FROM A POINT-INITIATED EXPLOSIVE CYLINDER, by D. Piacesi, jr. 13 Jan. 1967. 27p. charts, tables. NOSC task ORD-033-221/092-1/F008-08-11.
UNCLASSIFIED

With the use of the NOL two-dimensional hydrodynamics computer program (Cyclone), a detailed numerical analysis is made of the flow in the product gas of a detonating cylinder of pentolite (50/50 PETN/TNT) explosive. The explosive cylinder is initiated at a point on the central charge axis at one end-face.

1. Explosives - Hydrodynamics
2. Explosives - Detonation
I. Title
II. Piacesi, Dante, jr.
III. Project

Abstract card is unclassified.